



HAL
open science

Replication efficiency of rolling-circle replicon-based plasmids derived from porcine circovirus 2 in eukaryotic cells.

Florence Faurez, Daniel Dory, Aurélie Henry, Stéphanie Bougeard, André Jestin

► To cite this version:

Florence Faurez, Daniel Dory, Aurélie Henry, Stéphanie Bougeard, André Jestin. Replication efficiency of rolling-circle replicon-based plasmids derived from porcine circovirus 2 in eukaryotic cells.. *Journal of Virological Methods*, 2010, 165 (1), pp.27-35. 10.1016/j.jviromet.2009.12.013 . hal-00493407

HAL Id: hal-00493407

<https://ances.hal.science/hal-00493407>

Submitted on 18 Jun 2010

HAL is a multi-disciplinary open access archive for the deposit and dissemination of scientific research documents, whether they are published or not. The documents may come from teaching and research institutions in France or abroad, or from public or private research centers.

L'archive ouverte pluridisciplinaire **HAL**, est destinée au dépôt et à la diffusion de documents scientifiques de niveau recherche, publiés ou non, émanant des établissements d'enseignement et de recherche français ou étrangers, des laboratoires publics ou privés.

1
2
3
4
5
6
7
8
9
10
11
12
13
14
15
16
17
18
19
20
21
22

Replication efficiency of rolling-circle replicon-based plasmids derived from porcine circovirus 2 in eukaryotic cells

**Florence Faurez^a, Daniel Dory^{a*}, Aurélie Henry^a, Stéphanie Bougeard^b,
André Jestin^a**

^a French Food Safety Agency (AFSSA), Viral Genetics and Biosafety Unit, F-22440, Ploufragan, France

^b French Food Safety Agency (AFSSA), Epidemiology and Quality Assurance in Pig Production Research Unit, F-22440, Ploufragan, France

*Corresponding author: Daniel Dory, PhD, AFSSA (French Food Safety Agency), Viral Genetics and Biosafety Unit, BP-53, F-22440, Ploufragan, France

Phone: +33 2 96 01 64 42

Fax: +33 2 96 01 62 83

Email: d.dory@afssa.fr

23 **Replication efficiency of rolling-circle replicon-based plasmids derived from porcine**
24 **circovirus 2 in eukaryotic cells**

25

26 Abstract

27 In this study, a method was developed to measure replication rates of rolling-circle replicon-
28 based plasmids in eukaryotic cells. This method is based on the discriminative quantitation of
29 *Mbo*I-resistant, non-replicated input plasmids and *Dpn*I-resistant, replicated plasmids. To do
30 so, porcine circovirus type 2 (PCV2) replicon-based plasmids were constructed. These
31 plasmids contained the PCV2 origin of replication, the PCV2 Rep promoter and the PCV2
32 Rep gene. The results show that the replication rate depends on the length of the PCV2
33 replicon-based plasmid and not on the respective position of the Rep promoter and the
34 promoter of the gene of interest that encodes the enhanced green fluorescent protein (eGFP).
35 In all cases, it was necessary to add the Rep gene encoded by a plasmid and cotransfected as a
36 replication booster. This method can evaluate the replication potential of replicon-based
37 plasmids quickly and is thereby a promising tool for the development of plasmids for vaccine
38 purposes.

39

40 Keywords

41 Porcine Circovirus type 2 (PCV2); rolling-circle; replicon-based plasmid; quantitative PCR
42 assay; replication efficiency.

43

44 **1. Introduction**

45 Replicon-based plasmids derived from *Herpesviruses* (e.g. Epstein-Barr virus),
46 *Polyomaviruses* (e.g. BK virus, Simian virus 40), *Papillomaviruses* (e.g. bovine papilloma
47 virus 1), or *Geminiviruses* (e.g. bean yellow dwarf virus) have been developed recently for
48 gene expression and gene therapy (Kim et al., 2006; Mor et al., 2003; Shibata et al., 2005;
49 Van Craenenbroeck et al., 2000b). These plasmids contain a viral origin of replication and the
50 viral genes necessary for replication. Replicon-based plasmids have proved to be highly
51 valuable tools for: (1) producing high levels of proteins of interest in plants (Hefferon and
52 Fan, 2004; Mor et al., 2003); (2) delivering of therapeutic or complementing gene products
53 (Kim et al., 2006); (3) studying the regulation of replication (Takeda et al., 2005); and (4),
54 potentially, enhancing immune responses induced by DNA-based vaccines.

55 The porcine circovirus type 2 (PCV2), a member of the genus *Circovirus*, family
56 *Circoviridae*, contains a circular, single-stranded, positive-sense DNA genome which is about
57 1.8 kb in size. The intergenic region containing the origin of replication has a stem-loop
58 structure, which includes an octanucleotide sequence flanked by palindromes, and is bordered
59 by two open reading frames, ORF1 and ORF2. ORF1 is located on the positive strand and
60 encodes the Rep and Rep' proteins involved in replication initiation. ORF2 is located on the
61 negative strand of the intermediate double-stranded PCV2 genome that forms during
62 replication and it encodes the Cap protein, the capsid protein in PCV2 (Mankertz et al., 2004).
63 Owing to their ability to produce high levels of proteins in a short time, PCV2-based plasmids
64 may be valuable vectors for vaccine purposes compared to latent virus-based plasmids.
65 DNA replication of replicon-based plasmids in eukaryotic cells can be measured. The
66 replicated plasmid molecules can be distinguished from the initially transfected, input plasmid
67 molecules by their resistance to the *DpnI* restriction enzyme, which can only cleave DNA that
68 has been dam-methylated in bacteria. Thus, replicated plasmids can be detected by Southern

69 blotting (Mankertz et al., 1997) or by quantitative PCR (qPCR) (Baxter and McBride, 2005;
70 Taylor and Morgan, 2003). In comparison with Southern blotting, quantitative PCR is a
71 highly sensitive and quantitative method for detecting DNA replication and is significantly
72 faster (Taylor and Morgan, 2003).

73 For DNA-vaccine purposes, it is important to use a replicon-based plasmid — a so-called
74 replicative plasmid — that replicates rapidly to produce high quantities of vaccinating
75 proteins in a short time. However, little is known about the replication efficiency of
76 replicative plasmids. Replication efficiency can be estimated by comparing replicated
77 plasmids to the total number of extracted plasmids. In plasmids that undergo theta replication,
78 replication efficiency has been measured by comparing the number of plasmids after
79 incubation with and without DpnI (Takeda et al., 2005).

80 The difference between rolling-circle replication and theta replication is that rolling-circle
81 replicons replicate via a nicked-DNA intermediate and produce single-stranded DNA (Faurez
82 et al., 2009). The aim of the present study was to characterise a method to estimate the
83 efficiency of DNA replication of different rolling-circle, replicon-based plasmids using qPCR.
84 This information will be used to determine the replication rates of replicating plasmids and to
85 evaluate whether different primer pairs or different quantitative PCR protocols influence the
86 estimation of replication rates. PCV2 replicon-based plasmids were used as the rolling-circle
87 model.

88

89 **2. Materials and methods**

90 **2.1 Culture of PK15 cells**

91 Porcine circovirus type 1 (PCV1)-free porcine kidney (PK15) cells were grown in Eagle
92 minimal essential medium supplemented with 5% foetal bovine serum and 1% penicillin
93 (10 000 u/mL)-streptomycin (10 000 µg/mL) (Gibco, Invitrogen, Carlsbad, CA, USA) in 5%
94 CO₂ at 37°C and split 1:10 twice a week.

95

96 **2.2 Replicative and non-replicative plasmid constructs**

97 The pcDNA3 plasmid and the cloning vectors pCR4 and pBlueScript KS+ were obtained
98 from Invitrogen (Carlsbad, CA, USA). Five fragments were inserted into the plasmids (Figure
99 1a): (1) the enhanced green fluorescent protein (eGFP) reporter gene (GenBank accession no.
100 **U57609.1**); (2) the porcine circovirus type 2 (PCV2) OriRep fragment (GenBank accession
101 no. **AF201311**) that contains the Rep promoter, the origin of replication and ORF1 (Fig. 2);
102 (3) the cytomegalovirus immediate-early promoter (pCMV) of pcDNA3; (4) a PCR amplicon
103 obtained with oGVB2115 primers (Table 1) that contains a 1.3 kb fragment of the pBlueScript
104 KS+ vector flanked by a *KpnI* site; (5) a PCR amplicon from pcDNA3 obtained with
105 oGVB2117 primers (Table 1) that contains the beginning of the neomycin gene flanked by
106 *XmaI* and *MluI* sites.

107 In all, eleven plasmids were constructed for specific purposes (Fig. 1a). Two plasmids were
108 constructed to optimise the determination of the replication rate. A non-replicative plasmid
109 was obtained by inserting the pCMV and the eGFP reporter gene into pCR4 (pCR4-GFP). A
110 replicative plasmid was obtained by inserting PCV2 OriRep. The PCV2 OriRep fragment was
111 amplified by PCR from PCV2 (Fenaux et al., 2002) using the oGVB2100 primer pair (Table
112 1) and inserted into pCR4 (pCR4-Orirep). Then, to test the optimised determination method,
113 one non-replicative plasmid and three replicative plasmids were constructed. The non-

114 replicative plasmid was obtained by inserting the eGFP gene into pcDNA3 (pcDNA3-GFP).
115 For the replicative plasmids, the OriRep fragment was inserted at three different distances
116 from the CMV promoter in the pcDNA3 plasmid. The PCV2 OriRep fragment was amplified
117 by PCR from PCV2 using the oGVB2101 or the oGVB2106 primer pair (Table 1) and
118 inserted into pCR4. Each OriRep fragment was isolated from the pCR4 backbone by digestion
119 with specific restriction endonucleases, as indicated in Figure 1a, and inserted into the
120 pcDNA3-eGFP plasmid at 0.2kb (pOrirep0.2-GFP), 1.2kb (pOrirep1.2-GFP) or 3.2kb
121 (pOrirep3.2-GFP) from the CMV promoter. To study the influence of the promoter and
122 plasmid size on replication, five additional plasmids were constructed. Three of them were
123 derived from deletions within the replicative plasmid pOrirep0.2-GFP: deletion of the *SpeI*-
124 pCMV fragment (Fig. 1a pOrirep0.2-GFP CMV⁻); deletion of the *PsiI*-pSV40 neomycin
125 fragment (Fig. 1a pOrirep0.2-GFP SV40⁻); deletion of the *SpeI*-pCMV fragment and the *PsiI*-
126 pSV40 neomycin fragment (Fig. 1a pOrirep0.2-GFP CMV⁻/SV40⁻5.2kb). The latter plasmid,
127 which contained neither CMV nor SV40 promoters, was used to construct a plasmid with a
128 PCR amplicon obtained using oGVB2115 primers on pBluescript KS+ (pOrirep0.2-GFP
129 CMV⁻/SV40⁻6.5kb) . The fifth plasmid was a pBluescript KS+ plasmid with an *EcoRI*-OriRep
130 fragment from pCR4-Orirep, a *SpeI*-pCMV fragment from pcDNA3-GFP and a PCR
131 amplicon obtained using oGVB2117 primers on pcDNA3-GFP and cloned into the open
132 reading frame of pCMV (pKSOrirepCMVNeo) (Table 1).
133 *Escherichia coli* DH5α strain was transformed with each of the eleven plasmids. Plasmids
134 were purified using the NucleoSpin® plasmid kit (Macherey-Nagel, Düren, Germany)
135 according to the manufacturer's instructions and sequenced.

136

137 **2.3 Replication and replication-defective booster**

138 A pcDNA3.1 plasmid encoding the PCV2 ORF1 (Rep) called pcDNA3.1-Rep (Fig. 1b),
139 previously described and characterised in the AFSSA laboratory (Blanchard et al., 2003) was
140 used as a replication booster for the replicative plasmids. Replication of the PCV2 genome is
141 aborted if the tyrosine-96 of motif III of the Rep protein is substituted with phenylalanine-96.
142 However, the mutated Rep protein can still down-regulate the Rep promoter (Mankertz and
143 Hillenbrand, 2002; Steinfeldt et al., 2007). The mutation in motif III of the Rep protein was
144 introduced with the QuikChange XL site-directed mutagenesis kit (Stratagene-Agilent
145 Technologies, Waldbronn, Germany) according to the manufacturer's protocol using
146 pcDNA3.1-Rep as the template. The oGVB2112 primers used for mutagenesis are given in
147 Table 1. The mutation of the tyrosine-96 in the motif III sequence inhibits the digestion of
148 DNA by *Pst*I. The constructs were thus characterised by enzymatic restriction with *Pst*I and
149 constructs, which could not be digested by this enzyme, were sequenced to confirm the
150 sequence of Rep.

151

152 **2.4 Transfection of PK15 cells with PCV2-based replicative and non-replicative**
153 **plasmids**

154 Twenty-four hours before transfection, 4.5×10^5 of PK15 cells were plated onto 6-well tissue
155 culture plates. The final volume was 2 mL. For the quantitative real-time PCR-based
156 replication assay, 10 ng of plasmids were transfected to optimise the method and 10^9 copies of
157 plasmids were transfected to study the replication of different plasmids. The plasmids were
158 cotransfected with 1 µg of pcDNA3.1-Rep or pcDNA3.1-Rep mutated and, for reverse-
159 transcription PCR (RT-PCR), 1 µg of plasmids were transfected with Lipofectamine™ 2000
160 (Invitrogen, Carlsbad, CA, USA) according to the manufacturer's instructions.

161

2.5 Extraction of plasmids from transfected PK15 cells

Twenty-four hours after transfection the cells were scraped into 200 μ L of PBS 1X and lysed in protease and the lysis buffer provided with the QIAamp MinElute Virus Spin Kit (QIAGEN, Valencia, CA, USA) for 1 h at 56°C. Low-molecular-weight DNA was extracted with the QIAamp MinElute Virus Spin kit (QIAGEN, Valencia, CA, USA) according to the manufacturer's instructions. This kit was used because it has been described as being suitable for purifying single-stranded DNA (Ng et al., 2009). The DNA was resuspended in 100 μ L of H₂O. Plasmid extractions were performed under a DNA hood (Biocap™ DNA, Captair® bio, Erlab Biocapt).

2.6 Quantitative real-time PCR-based replication assay

The quantitative real-time PCR-based replication assay was based on the methylation status of plasmids transfected into eukaryotic cells. Methylation status depends on whether or not replication has occurred within eukaryotic cells. Dam-methylation of the GATC site occurs in input plasmids (i.e. generated in prokaryotic (bacterial) cells), whereas the GATC site is not methylated in plasmids that replicate in eukaryotic cells. Therefore, to differentiate replicated from non-replicated plasmids, low-molecular-weight DNA extracted from PK15 cells was incubated either with *DpnI* that cuts the dam-methylated GATC site or with *MboI* that, on the contrary, cuts the non-methylated GATC site. To reduce the background level that is observed in quantitative real-time PCR due to incompletely digested DNA, Exonuclease III (ExoIII) was added to digest any incompletely cut DNA (Taylor and Morgan, 2003). ExoIII is an exodeoxyribonuclease that does not act on intact circular plasmids, but rather digests one strand of duplex DNA at a blunt end, at a 5' overhang or at internal nicks. The enzyme acts in a 3' \rightarrow 5' direction and produces stretches of single-stranded DNA (Rogers and Weiss, 1980;

186 Weiss, 1976). The conditions of digestion used were those described previously (Morgan and
187 Taylor, 2005).

188 In preliminary experiments, TaqMan and SYBR Green real-time PCR assays were compared.
189 The SYBR Green protocol was used in for the rest of the study. Primer pairs and probes
190 indicated in Table 1 were designed using Primer Express™ Software (Applied Biosystems,
191 Foster City, USA). Quantitative PCR was performed in an ABI Prism 7000 SDS (Applied
192 Biosystems, Foster City, USA) in a 25 µL total volume containing 1 X Universal Master Mix
193 or 1 X SYBR Green Master Mix (Applied Biosystems, Foster City, USA), 300 nM each
194 primer, 200 nM probe for the TaqMan protocol and 2 µL of digested DNA. After 2 min at
195 50°C and incubation for 10 min at 94°C, 40 PCR cycles consisting of a 15 sec denaturing step
196 at 94°C and a 1 min annealing/extension step at 60°C were performed. Plasmid copy numbers
197 were determined by analysing a standard DNA curve ranging from 10⁸ to 10¹ plasmid copies.
198 The PCR experiments were performed twice using nine replicates for statistical analysis or
199 twice in duplicate in the rest of the study. Data were analysed using Sequence Detection
200 Software version 1.2.3 (Applied Biosystems, Foster City, USA).

201

202 **2.7 RNA extraction and reverse-transcription PCR**

203 Twenty-four hours after transfection, total RNA was extracted from PK15 cells using the
204 TRIzol® reagent according to the manufacturer's instructions (Invitrogen, Carlsbad, CA,
205 USA). Plasmids were present in the same phase as RNA. To eliminate plasmids, 5 µL of total
206 RNA was incubated with RNase-free DNase as indicated by the manufacturer (QIAGEN,
207 Valencia, CA, USA). Then, 15 µL of DNA-free RNA was reverse-transcribed to cDNA with
208 random primers using the high-capacity cDNA archive kit according to the manufacturer's
209 instructions (Applied Biosystems, Foster City, USA). The cDNA was used immediately or
210 stored at -20°C until use. To differentiate Rep RNA from Rep' RNA, intron-flanking primers

211 were used (Table 1: 98_F and oGVB2118_R). The amplicon size was 774pb and 391pb for
212 Rep cDNA and Rep' cDNA, respectively. β -actin cDNA was used as an internal control. The
213 PCR reaction was performed in a total volume of 50 μ L containing 10 μ L of cDNA, 10 μ L of
214 5X Green GoTaq buffer, 0.2 μ M 98_F and oGVB2118_R primers, 0.2 μ M each dNTP and 1
215 unit of GoTaq® Flexi DNA polymerase (Promega, Southampton, UK) using the G-STORM
216 GS1 system (Genetic Research Instrumentation, Braintree, Essex, UK). Thermal cycle
217 conditions were as follows: 94°C for 5 min followed by 30 cycles at 94°C for 30 sec, 59°C for
218 30 sec, 72°C for 1 min with a final extension of 72°C for 10 min. Amplicons were visualised
219 by 2% agarose gel electrophoresis and ethidium bromide staining.

220

221 **2.8 Statistics**

222 The aim of the statistical analysis was to test in each population, i.e. non-replicative and
223 replicative plasmids, the difference between the quantity of DNA incubated with ExoIII only
224 (qE) and the sum of the quantity of DNA incubated with *DpnI* and ExoIII (qDE) and *MboI*
225 and ExoIII (qME). Two-tailed Student *t*-tests were used and computed using Systat 9.0
226 software. The associated power of the Student *t*-tests was computed with the POWER
227 procedure of SAS software (SAS, 2004). The quantities of plasmids in digested DNA samples
228 were considered to be different if the Type I error was less than 5% and considered to be
229 similar if the Type II error was less than 20%, i.e. a power higher greater than 80%, for an
230 associated Type I error at 5% (Jenny, 2001; Melot, 2003). The Mann-Whitney test was used
231 for comparisons of differences in the results of real-time PCR on two different amplification
232 targets and in the results of real-time PCR using the TaqMan probe or SYBR Green.

233 3. Results

234 3.1 Optimisation of the replication rate calculation

235 In this study, the replication rate was defined as the percentage of replicated plasmids at 24 h
236 post-transfection. To evaluate the replication rate of plasmids, a quantitative real-time PCR-
237 based assay was developed to quantify input plasmids or replicated plasmids, but not the
238 cotransfected pcDNA3.1-Rep replication booster. To do so, the PCR primers targeted a
239 GATC site and this site is not present in pcDNA3.1-Rep. In theory, the quantity of plasmids
240 after incubation with ExoIII (qE) should be equal to the sum of the quantity of plasmids
241 incubated with *DpnI* and ExoIII and the quantity of plasmids incubated with *MboI* and ExoIII
242 (qDE+qME). Consequently, the replication rate can be calculated using qE or qDE+qME as
243 the denominator.

244 To test this assumption, the number of plasmid copies of pCR4-GFP and of pCR4-Orirep
245 were quantified. Visually, qE did not appear different from qDE+qME (Fig. 3). In the case of
246 pCR4-GFP, statistics showed that qE and qDE+qME were not significantly different
247 ($p=0.766$). However, these two groups were not shown to be similar, because the Type II
248 error was greater than 20%. To conclude on similarity at a Type II error of 20%, quantitative
249 PCR must be performed 1526 times for each type of plasmid. In the case of pCR4-Orirep,
250 statistical tests showed that qE and qDE+qME were significantly different ($p=0.017$).

251 Therefore, the assumption could not be validated for replicative plasmids. The replication rate
252 of replicative plasmids incubated with *MboI* and ExoIII exceeded 100% when using qE as the
253 denominator in the calculation (data not shown). qME and qDE had the same conditions of
254 digestion; thus the replication rate was calculated using $qDE/(qME+qDE)$.

255

256 **3.2 Detection of Rep and Rep' mRNA production**

257 Reverse-transcription PCR was used to analyse the transcription of Rep and Rep' proteins
258 encoded by pOrirep0.2-GFP or by pcDNA3.1-Rep. Reverse-transcription PCR amplified two
259 cDNA fragments corresponding to the Rep mRNA (774pb) and to the spliced mRNA of Rep'
260 (391pb) for pOrirep0.2-GFP and for pcDNA3.1-Rep (Fig. 4). These bands were not present in
261 the cDNA controls of PK15 cells that were not transfected or that were transfected by non-
262 replicative pcDNA3. Thus, the expression of both Rep and Rep' could be detected.

263

264 **3.3 Necessity of cotransfection with pcDNA3.1-Rep to show the replication rate in**
265 **vitro**

266 In preliminary experiments pCR4-GFP or pCR4-Orirep were transfected in PK15 cells
267 without the replication booster pcDNA3.1-Rep. The mean replication rate of pCR4-Orirep
268 was similar to that of pCR4-GFP (data not shown). The cotransfection of pcDNA3.1-Rep
269 resulted in a replication rate of 49% for pCR4-Orirep (Fig. 5). If the Rep gene of pcDNA3.1-
270 Rep was mutated, the replication rate of pCR4-Orirep returned to the background level. No
271 replication was observed for pCR4-GFP, even in the presence of pcDNA3.1-Rep.

272

273 **3.3 Replication rates determined with two different quantitative real-time PCR**
274 **methods and for two different amplification targets**

275 Plasmid replication rates were compared for two primer pairs associated with a TaqMan probe
276 or with the SYBR Green dye. The quantitative real-time PCR-based replication assays were
277 tested with pcDNA3-GFP and pOrirep0.2-GFP (Fig. 1a); each plasmid was cotransfected with
278 pcDNA3.1-Rep. One primer pair was situated in the neomycin gene with a GATC site located
279 in the middle of the amplicon, and the other primer pair was placed at the junction of the GFP
280 gene and the pcDNA3 backbone with a GATC site located in the reverse primer (Fig. 6a).
281 Neither the quantity of plasmids evaluated by the formula $q_{DE}+q_{ME}$ (Fig. 6b) nor the

282 replication rates (Fig. 6c) were significantly different, whatever the primer pair. This was
283 verified for pcDNA3-GFP and pOrirep0.2-GFP (Fig. 6b and 6c). Moreover, the use of a
284 TaqMan probe or a SYBR Green dye (Fig. 7a) did not introduce significant variation in the
285 quantity of plasmids measured (Fig. 7b) or in the mean replication rates (Fig. 7c) of either
286 construct.

287

288 **3.4 Example application: mean replication rate of PCV2-based replicons in PK15** 289 **cells 24 h post-transfection**

290 PCV2-based replicons were cotransfected with pcDNA3.1-Rep into PK15 cells. The non-
291 replicative plasmids have a mean background replication rate below 5% (Fig. 8). pCR4-
292 Orirep showed a mean replication rate of $63\% \pm 8\%$. The mean replication rates of the three
293 replicative plasmids encoding the eGFP gene were lower, i.e. $14\% \pm 2\%$, $13\% \pm 3\%$ and 12%
294 $\pm 2\%$ for pOrirep1.2-GFP, pOrirep0.2-GFP and pOrirep3.2-GFP, respectively. Compared to
295 the three replicative eGFP encoding plasmids, pCR4-Orirep was smaller (5.2kb vs. 7.4kb) and
296 did not contain strong eukaryotic promoters such as pCMV and pSV40.

297 **3.5 Mean replication rate depended on plasmid size, but not on the presence of** 298 **strong eukaryotic promoters**

299 To determine whether the size of the plasmid or the presence of strong eukaryotic promoters
300 could modify the mean replication rates of the PCV2-based replicons, five additional plasmids
301 were constructed and tested. Plasmids with or without eukaryotic promoters and greater than
302 5.9 kb in size still had low mean replication rates. On the contrary, 5.2 kb plasmids with or
303 without eukaryotic promoters had replication rates of about the same magnitude as pCR4-
304 Orirep (Fig. 8).

305

306 **4. Discussion**

307 In this study, a rapid, quantitative real-time PCR-based assay was developed to measure the
308 replication rates of PCV2-based replicons. The replication rate was defined as the percentage
309 at 24 h post-transfection of the number of replicated plasmids compared to the total number of
310 plasmids present in the cells (i.e. replicated and initial input plasmids). The choice of the
311 *Escherichia coli* strain in which replicon-based plasmids were produced was important. For
312 example, the *E. coli* TOP10 strain has more mutations in the system of methylation and
313 restriction (hsdRMS gene) than the DH5 α strain; this difference caused an increase in the
314 replication rate (data not shown). Primers for short PCR amplicons containing a GATC
315 sequence were designed to discriminate between replicated and non-replicated plasmids after
316 incubation in eukaryotic cells. A plasmid encoding the PCV2 Rep protein (pcDNA3.1-Rep)
317 was needed to boost and to detect the in vitro replication of the PCV2-based replicons.
318 Comparable replication rates were determined using two different amplification targets. The
319 use of a specific TaqMan probe and amplicon detection using SYBR Green dye also resulted
320 in comparable replication rates.

321 As in theta replication, rolling-circle replication is a semi-conservative replication system.
322 However, a rolling-circle replicon replicates via a nicked DNA intermediate and produce
323 single-stranded DNA (Faurez et al., 2009). The present study showed that the quantity of
324 plasmids after incubation with ExoIII (qE) and the sum of the quantity of plasmids after
325 incubation with *DpnI* and ExoIII plus the quantity of plasmids after incubation with *MboI* and
326 ExoIII (qDE+qME) were significantly different in replicative plasmids. This difference may
327 be due to the products of rolling-circle replication, namely single-stranded DNA and nicked
328 DNA. In contrast to viruses that replicate via rolling-circle replication, rolling-circle replicon-
329 based plasmids do not encode the capsid protein which up-regulates the amount of single-
330 stranded DNA by protecting viral DNA from host proteins (Padidam et al., 1999).

331 Consequently single-stranded DNA probably did not contribute to the difference between qE
332 and qDE+qME. On the contrary, nicked plasmids may have an impact on the number of
333 plasmid copies detected by quantitative real-time PCR. The efficiency of ExoIII digestion
334 may vary with the quantity of nicked DNA and digested DNA (Hoheisel, 1993). The qME to
335 qE ratio exceeded 100%: more DNA was detected when DNA was incubated with *MboI* and
336 ExoIII than with ExoIII only. The difference in the quantity of plasmids detected by
337 quantitative real-time PCR may be due to the complete digestion of nicked DNA in qE but not
338 in qME. ExoIII may digest all the double-stranded plasmids and produce single-stranded
339 DNA, thereby decreasing the number of plasmid copies detected by quantitative real-time
340 PCR. Because qDE and qME had the same conditions of digestion, qDE+qME was used to
341 calculate the replication rate instead of qE. Hemi-methylated plasmids are cleaved by *DpnI*
342 under conditions of enzyme excess, long digestion times or small quantities of DNA template
343 (Lu et al., 2002) but are not cleaved by *MboI* (Stancheva et al., 1999). Thus, hemi-methylated
344 plasmids are not amplified by PCR, resulting in a possible underestimation of the replication
345 rate. To be detected, replication of plasmids had to be sufficient for detection by real-time
346 PCR assays.

347 This method made it possible to differentiate the replication efficiency of different plasmids.
348 In this study, non-replicative plasmids showed a background level lower than 10% of the
349 mean replication rate in all the experiments. This background level could be explained by a
350 percentage of input DNA that becomes *DpnI*-resistant (Takeda et al., 2005). In this study,
351 mean replication rates could only be determined when the replicative plasmids were
352 cotransfected with pcDNA3.1-Rep. There are two possible explanations for this result: (1) the
353 replicative plasmids could not replicate because Rep and/or Rep' proteins were not produced,
354 or (2) the replication rate was too low to be detected because only low quantities of Rep
355 and/or Rep' proteins were produced. The first explanation can be discounted because it was

356 shown that the Rep gene and Rep promoter had not mutated and that the Rep gene was indeed
357 transcribed. However, dysfunction may be caused by the low production of Rep and Rep' or
358 down-regulation of the Rep promoter. It has been reported that transcriptional interference
359 with Epstein-Barr virus-derived vectors depends on the thymidine kinase promoter in the
360 episomal vector (Van Craenenbroeck et al., 2003). However, in eukaryotic cells, the Rep
361 promoter could not be perturbed by the presence of the immediate early CMV promoter or the
362 SV40 promoter in the plasmid because pCR4-Orirep did not contain these eukaryotic
363 promoters. Furthermore, the Rep promoter may not be exchanged with another promoter
364 because it is down-regulated by the Rep protein (Mankertz and Hillenbrand, 2002) which
365 limits the toxicity of Rep on cells. This down-regulation may rapidly decrease the production
366 of proteins and also replication.

367 pCR4-Orirep seemed to replicate more rapidly than pOrirep0.2-GFP, pOrirep1.2-GFP and
368 pOrirep3.2-GFP. The differences between replicative plasmids were (1) the size of the
369 plasmids, with 5.2 kb for pCR4-Orirep and 7.3 or 7.4 kb for pOrirep0.2-GFP, pOrirep1.2-GFP
370 and pOrirep3.2-GFP and (2) although pOrirep0.2-GFP, pOrirep1.2-GFP and pOrirep3.2-GFP
371 contained strong eukaryotic promoters, pCR4-Orirep did not. Strong promoter-enhancers such
372 as the CMV immediate-early gene enhancer interfere with the origin of replication of SV40
373 (Chen et al., 2000) and oversized vectors, such as BKV replicon plasmids, are more subject to
374 recombination events which may lead to defective replication (Van Craenenbroeck et al.,
375 2000a). The present study showed that size had an impact on the replication rate of rolling-
376 circle replicon-based plasmids, since plasmids with a size of around 5.2 kb replicated at a high
377 rate and plasmids with larger sizes replicated at lower rates. Prokaryotic rolling-circle
378 replicons generate high-molecular-weight DNA during replication in prokaryotic cells when a
379 fragment is inserted into the replicon (Dabert et al., 1992; Gruss and Ehrlich, 1988). It is
380 possible that replication of PCV2 replicon-based plasmids was initiated, but that replication

381 could not be terminated due to the large plasmid size, thereby affecting the replication rate. In
382 this study, the strong eukaryotic promoters pCMV and pSV40 did not affect the replication
383 rates.

384 In conclusion, the method described in this study made it possible to calculate plasmid
385 replication rates in eukaryotic cells and to compare different rolling-circle replicons. Using
386 this method, the influence of plasmid size, the presence of strong eukaryotic promoters and
387 the location of the OriRep sequence in the plasmid were studied. This method should be
388 useful for rolling-circle or theta replicons, and in particular for studying the regulation of
389 replicon or virus replication. The quantitative real-time PCR assay reported here could also
390 advantageously be used to evaluate the replication potential of replicon-based plasmids
391 developed for vaccine purposes. Unlike gene therapy, the replicon-based plasmids have to
392 replicate rapidly to produce large amounts of the encoded proteins of interest in a short time.

393

394

395 **Acknowledgements**

396 This study was partially supported by grants from the European Commission (Epizone
397 Network of Excellence, Contract No. FOODCT-2006-016236). The authors are grateful to
398 Béatrice Grasland, Yannick Blanchard, Anne-Cécile Nignol (AFSSA, Ploufragan, France)
399 and Prof. Iain Morgan (University of Glasgow, UK) for their advice.

400

401 **References**

- 402
- 403
- 404 Baxter, M.K., McBride, A.A., 2005. An acidic amphipathic helix in the Bovine
405 Papillomavirus E2 protein is critical for DNA replication and interaction with the E1
406 protein. *Virology* 332, 78-88.
- 407 Blanchard, P., Mahe, D., Cariolet, R., Keranflec'h, A., Baudouard, M.A., Cordioli, P., Albina,
408 E., Jestin, A., 2003. Protection of swine against post-weaning multisystemic wasting
409 syndrome (PMWS) by porcine circovirus type 2 (PCV2) proteins. *Vaccine* 21, 4565-
410 75.
- 411 Chen, P.H., Tseng, W.B., Chu, Y., Hsu, M.T., 2000. Interference of the simian virus 40 origin
412 of replication by the cytomegalovirus immediate early gene enhancer: evidence for
413 competition of active regulatory chromatin conformation in a single domain. *Mol.*
414 *Cell. Biol.* 20, 4062-74.
- 415 Dabert, P., Ehrlich, S.D., Gruss, A., 1992. High-molecular-weight linear multimer formation
416 by single-stranded DNA plasmids in *Escherichia coli*. *J. Bacteriol.* 174, 173-8.
- 417 Faurez, F., Dory, D., Grasland, B., Jestin, A., 2009. Replication of porcine circoviruses. *Virology*
418 *J.* 6, 60.
- 419 Fenaux, M., Halbur, P.G., Haqshenas, G., Royer, R., Thomas, P., Nawagitgul, P., Gill, M.,
420 Toth, T.E., Meng, X.J., 2002. Cloned genomic DNA of type 2 porcine circovirus is
421 infectious when injected directly into the liver and lymph nodes of pigs:
422 characterization of clinical disease, virus distribution, and pathologic lesions. *J. Virol.*
423 76, 541-51.
- 424 Gruss, A., Ehrlich, S.D., 1988. Insertion of foreign DNA into plasmids from gram-positive
425 bacteria induces formation of high-molecular-weight plasmid multimers. *J. Bacteriol.*
426 170, 1183-90.
- 427 Hefferon, K.L., Fan, Y., 2004. Expression of a vaccine protein in a plant cell line using a
428 geminivirus-based replicon system. *Vaccine* 23, 404-10.
- 429 Hoheisel, J.D., 1993. On the activities of *Escherichia coli* exonuclease III. *Anal. Biochem.*
430 209, 238-46.
- 431 Jenny, J.Y., 2001. [Beta risk: an unrecognized risk of statistical error]. *Rev. Chir. Orthop.*
432 *Reparatrice Appar. Mot.* 87, 170-2.
- 433 Kim, Y.D., Park, K.G., Morishita, R., Kaneda, Y., Kim, S.Y., Song, D.K., Kim, H.S., Nam,
434 C.W., Lee, H.C., Lee, K.U., Park, J.Y., Kim, B.W., Kim, J.G., Lee, I.K., 2006. Liver-
435 directed gene therapy of diabetic rats using an HVJ-E vector containing EBV plasmids
436 expressing insulin and GLUT 2 transporter. *Gene Ther.* 13, 216-24.
- 437 Lu, L., Patel, H., Bissler, J.J., 2002. Optimizing DpnI digestion conditions to detect replicated
438 DNA. *Biotechniques* 33, 316-8.
- 439 Mankertz, A., Caliskan, R., Hattermann, K., Hillenbrand, B., Kurzendoerfer, P., Mueller, B.,
440 Schmitt, C., Steinfeldt, T., Finsterbusch, T., 2004. Molecular biology of Porcine
441 circovirus: analyses of gene expression and viral replication. *Vet. Microbiol.* 98, 81-8.
- 442 Mankertz, A., Hillenbrand, B., 2002. Analysis of transcription of Porcine circovirus type 1. *J.*
443 *Gen. Virol.* 83, 2743-51.
- 444 Mankertz, A., Persson, F., Mankertz, J., Blaess, G., Buhk, H.J., 1997. Mapping and
445 characterization of the origin of DNA replication of porcine circovirus. *J. Virol.* 71,
446 2562-6.

447 Melot, C., 2003. [What does "power of the study" mean? How to compute the power of a
448 study? How to compute the number of subjects needed for a trial?]. *Rev. Mal. Respir.*
449 20, 602-3.

450 Mor, T.S., Moon, Y.S., Palmer, K.E., Mason, H.S., 2003. Geminivirus vectors for high-level
451 expression of foreign proteins in plant cells. *Biotechnol. Bioeng.* 81, 430-7.

452 Morgan, I.M., Taylor, E.R., 2005. Detection and quantitation of HPV DNA replication by
453 Southern blotting and real-time PCR. *Methods Mol. Med.* 119, 349-62.

454 Ng, T.F., Manire, C., Borrowman, K., Langer, T., Ehrhart, L., Breitbart, M., 2009. Discovery
455 of a novel single-stranded DNA virus from a sea turtle fibropapilloma by using viral
456 metagenomics. *J. Virol.* 83, 2500-9.

457 Padidam, M., Beachy, R.N., Fauquet, C.M., 1999. A phage single-stranded DNA (ssDNA)
458 binding protein complements ssDNA accumulation of a geminivirus and interferes
459 with viral movement. *J. Virol.* 73, 1609-16.

460 Rogers, S.G., Weiss, B., 1980. Exonuclease III of *Escherichia coli* K-12, an AP endonuclease.
461 *Methods Enzymol.* 65, 201-11.

462 Shibata, M.A., Miwa, Y., Miyashita, M., Morimoto, J., Abe, H., Otsuki, Y., 2005.
463 Electrogenic transfer of an Epstein-Barr virus-based plasmid replicon vector containing
464 the diphtheria toxin A gene suppresses mammary carcinoma growth in SCID mice.
465 *Cancer Sci.* 96, 434-40.

466 Stancheva, I., Koller, T., Sogo, J.M., 1999. Asymmetry of Dam remethylation on the leading
467 and lagging arms of plasmid replicative intermediates. *Embo J.* 18, 6542-51.

468 Steinfeldt, T., Finsterbusch, T., Mankertz, A., 2007. Functional analysis of cis- and trans-
469 acting replication factors of porcine circovirus type 1. *J. Virol.* 81, 5696-704.

470 Takeda, D.Y., Shibata, Y., Parvin, J.D., Dutta, A., 2005. Recruitment of ORC or CDC6 to
471 DNA is sufficient to create an artificial origin of replication in mammalian cells.
472 *Genes Dev.* 19, 2827-36.

473 Taylor, E.R., Morgan, I.M., 2003. A novel technique with enhanced detection and
474 quantitation of HPV-16 E1- and E2-mediated DNA replication. *Virology* 315, 103-9.

475 Van Craenenbroeck, K., Vanhoenacker, P., Duchau, H., Haegeman, G., 2000a. Molecular
476 integrity and usefulness of episomal expression vectors derived from BK and Epstein-
477 Barr virus. *Gene* 253, 293-301.

478 Van Craenenbroeck, K., Vanhoenacker, P., Haegeman, G., 2000b. Episomal vectors for gene
479 expression in mammalian cells. *Eur. J. Biochem.* 267, 5665-78.

480 Van Craenenbroeck, K., Vanhoenacker, P., Roman, I., Haegeman, G., 2003. Orientation-
481 dependent gene expression with Epstein-Barr virus-derived vectors. *FEBS Lett.* 555,
482 489-94.

483 Weiss, B., 1976. Endonuclease II of *Escherichia coli* is exonuclease III. *J. Biol. Chem.* 251,
484 1896-901.

485
486

487 **Figure captions, tables, figures, schemes**

488

489 Figure 1a: Representation of replicative and non-replicative plasmids. From left to right:
490 backbones, non-replicative plasmids and replicative plasmids. Light grey arrow: eGFP
491 reporter gene; black arrow with a stem-loop: PCV2 OriRep; dark grey arrow: IE CMV
492 promoter; black arrow: PCR amplicon obtained with oGVB2115 primers (Table 1); white
493 arrow: PCR amplicon obtained with oGVB2117 primers (Table 1).

494

495 Figure 1b: Representation of the replication booster used in this study, pcDNA3.1-Rep. The
496 backbone is pcDNA3.1 zeo+.

497

498 Figure 2: PCV2 fragment used to render plasmids replicative. The PCV2 genome is
499 represented on the left. It contains ORF1 (in black), ORF2 (in grey) and an origin of
500 replication (stem loop). The OriRep fragment is boxed.

501

502 Figure 3: Quantitation of plasmids by real-time PCR-based replication assay. Non-replicative
503 plasmid, pCR4-GFP; replicative plasmid, pCR4-Orirep. Plasmids were cotransfected with
504 pcDNA3.1-Rep. Total plasmids, quantity of plasmids incubated with ExoIII; quantity of non-
505 replicated plasmids + replicated plasmids, quantity of plasmids incubated with *DpnI* and
506 ExoIII plus quantity of plasmids incubated with *MboI* and ExoIII. The real-time PCR
507 experiments were carried out twice using nine replicates ; standard error bars are shown.

508

509 Figure 4: Detection of Rep and Rep' mRNAs 24 h post-transfection in a non-replicative
510 plasmid, a replicative plasmid and a plasmid encoding the Rep gene. Lane 1: non-transfected
511 PK15 cells; lane 2: PK15 cells transfected by pcDNA3-GFP; lane 3: PK15 cells transfected
512 by pOrirep0.2-GFP; lane 4: PK15 cells transfected by pcDNA3.1-Rep. Results for β -actin
513 mRNA, used as a positive control, are shown.

514

515 Figure 5: Need for a plasmid which expresses Rep protein at high levels. pCR4-GFP or
516 pCR4-Orirep were cotransfected into PK15 cells with a pcDN3.1-Rep, or they were
517 cotransfected with pcDN3.1-Rep mutated. The replication rates were calculated as described
518 above. The real time-PCR experiments were carried out twice in duplicate and the standard
519 error bars are shown.

520

521 Figure 6: Influence of the two primer pairs designed for the quantitative real time-PCR on the
522 determination of the replication rates. The real-time-PCR-based replication assays were tested
523 with two primer pairs and pcDNA3-GFP and pOrirep0.2-GFP were both cotransfected with
524 pcDN3.1-Rep. a) Representation of the primer pairs b) Quantity of plasmids depending on the
525 primers used. c) Mean replication rate for non-replicative and replicative plasmids for each
526 primer pairs. The real time-PCR experiments were carried out twice in duplicate and the
527 standard error bars are given. The Mann-Whitney test was used to compare differences
528 between results.

529

530 Figure 7: Influence of the real time-PCR method on the determination of the replication rates.
531 The real-time-PCR-based replication assays were tested with TaqMan probe 2111 or SYBR
532 Green dye. pcDNA3-GFP and pOrirep0.2-GFP, both cotransfected with pcDN3.1-Rep, were
533 used. a) Representation of the two quantitative real-time PCR methods b) Quantity of
534 plasmids after real time-PCR with the TaqMan probe or the SYBR Green dye. c) Mean rate of
535 replication after real time-PCR with the TaqMan probe or the SYBR Green dye. The real-time

536 PCR experiments were carried out twice in duplicate and the standard error bars are shown.
537 The Mann-Whitney test was used to compare differences between results.

538

539 Figure 8: Mean replication rates for PCV2 replicons 24 h post-transfection. Plasmids were
540 cotransfected into PK15 cells with pcDN3.1-Rep. Replication rates were calculated as
541 described in 3.1. The quantitative real-time PCR experiments were carried out twice in
542 duplicate and the standard error bars are shown.

543

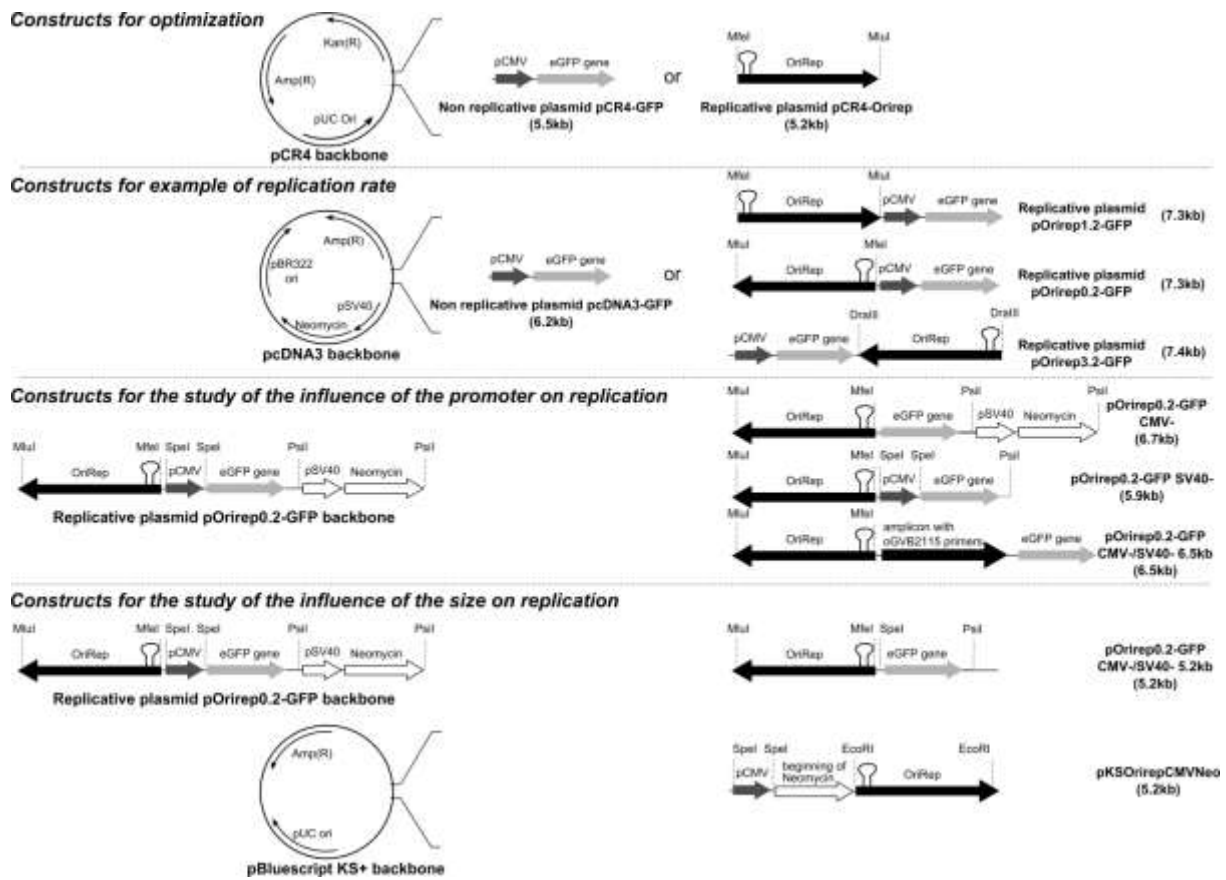
544
545
546
547

Table 1: Primer and probe sequences for construction of plasmids, for real-time PCR and for reverse transcriptase PCR

name	function	Specificity	size of amplicon	sequence
oGV82100_F	cloning	MfeI CAATTG	1231pb	5'-CAATTGCGGGTGTGAAGATGCCATT-3'
oGV82100_R	cloning	MluI ACGCGT		5'-ACGCGTCCCACTTAACCCCTAATGA-3'
oGV82101_F	cloning	MluI ACGCGT	1231pb	5'-ACGCGTGGGTGTGAAGATGCCATT-3'
oGV82101_R	cloning	MfeI CAATTG		5'-CAATTGCGCCCACTTAACCCCTAATGA-3'
oGV82107_F	cloning	DraIII CACGTAGTG	1231pb	5'-CACGTAGTGCCACTTAACCCCTAATGAAT-3'
oGV82106_R	cloning	DraIII CACGTAGTG		5'-CACTACGTGTGTGAAGATGCCATTTTTC-3'
oGV82115_F	cloning	KpnI GGTAAC in the end of ampicillin gene	1273pb	5'-GGTACCGTCTATTTGTTTCATCCATAG-3'
oGV82115_R	cloning	KpnI GGTAAC in the middle of f1 origin		5'-GGTACCTCAAGCTCTAAATCGGG-3'
oGV82117_F	cloning	XbaI CCCGGG in the beginning of neomycin gene	430pb	5'-CCCGGGCATGATTGAAACAAGATG-3'
oGV82117_R	cloning	MluI ACGCGT in the middle of neomycin gene		5'-ACGCGTAGTACGTGCTCCTCGAT-3'
oGV82112_F	mutagenesis	mutations Y ₈₈ in F ₈₈ and S ₈₈ in A ₈₈	/	5'-ACTCCATCAGTAAGTTCCTTTAGCGCAAAATCTTATTCTGCTGATCTGTCC-3'
oGV82112_R	mutagenesis	mutations Y ₈₈ in F ₈₈ and S ₈₈ in A ₈₈	/	5'-GGAACAGATCAGCAGAAATAAGAAATTTGCGCTAAAGAAGGCAACTACTGATGGAGT-3'
oGV82111_F	qPCR assay	in the GFP gene	amplicon of 93pb and DpnI site in the middle	5'-GCATGGACGAGCTGTACAAGTAA-3'
oGV82111_R	qPCR assay	in the backbone of pCDNA3	site in the middle	5'-ATCAGCGAGCTCTAGCATTTAGG-3'
oGV82113_F	qPCR assay	in the neomycin gene	amplicon of 92pb DpnI site	5'-GCTCCTGCCGAGAAAGTATCC-3'
oGV82113_R	qPCR assay	in the neomycin gene	in reverse primer	5'-TTCGCTTGGTGGTCCGAATG-3'
88_F	RT PCR Rep'	in the beginning of Rep gene	amplicon of Rep' = 774pb	5'-GTGGGTGTTCACTCGAATAA-3'
oGV82118_R	RT PCR Rep'	after the end of intron of flap gene	amplicon of Rep' = 391pb	5'-AGAGCTTCTACAGCTGGGACA-3'
probe 2111	probe qPCR assay	FAM-MGB	/	5'-CTCAGCATGCACTCA-3'
Bactine forward	RT PCR Bactine	/	64pb	5'-GATCGTGGCGGACATCAAG-3'
Bactine reverse	RT PCR Bactine	/		5'-GGCCATCTCCTGCTCGAA-3'

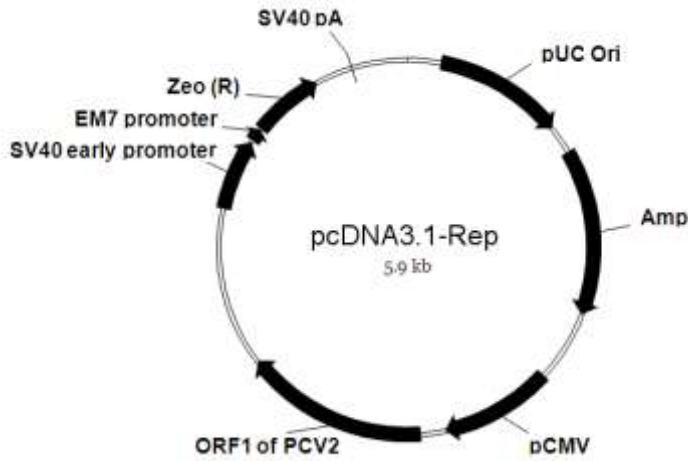
548
549
550
551

552
553



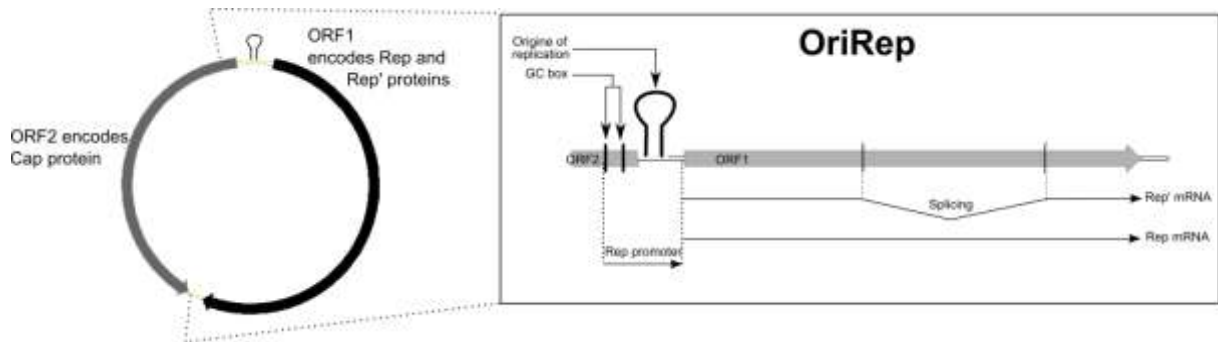
554
555
556

Figure 1a



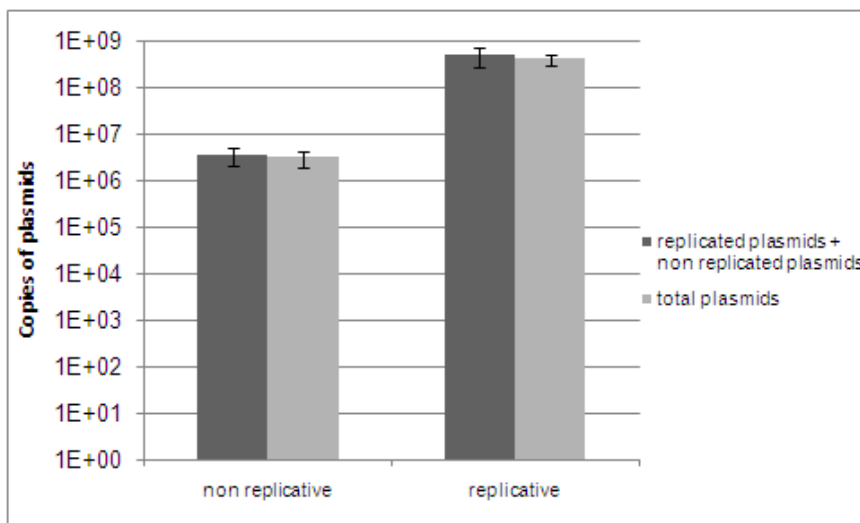
557
558
559

Figure 1b



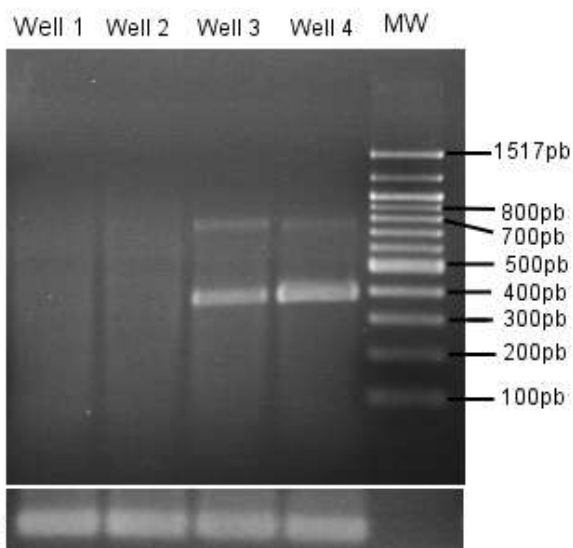
560
561 Figure 2

562
563
564
565



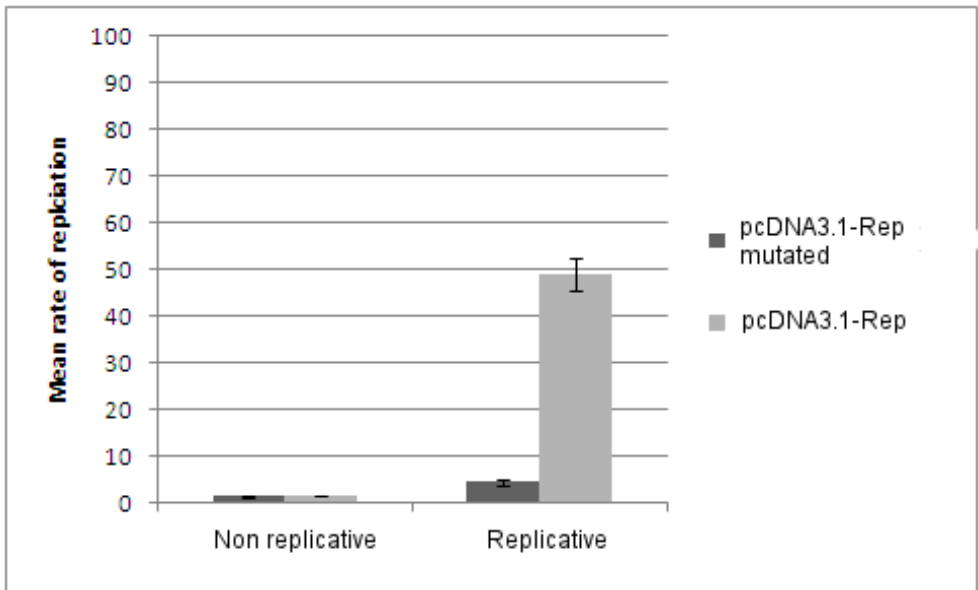
566
567 Figure 3

568
569
570
571

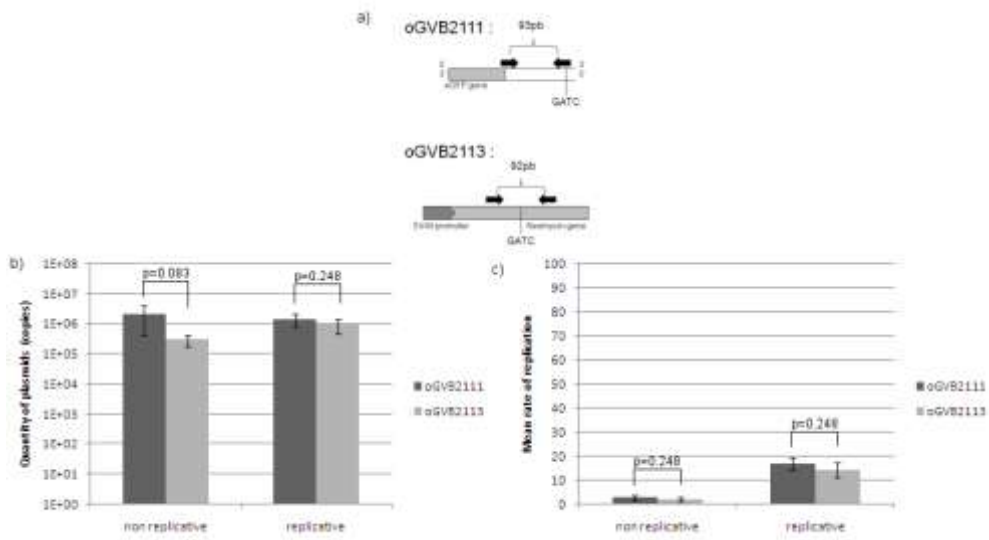


572
573 Figure 4

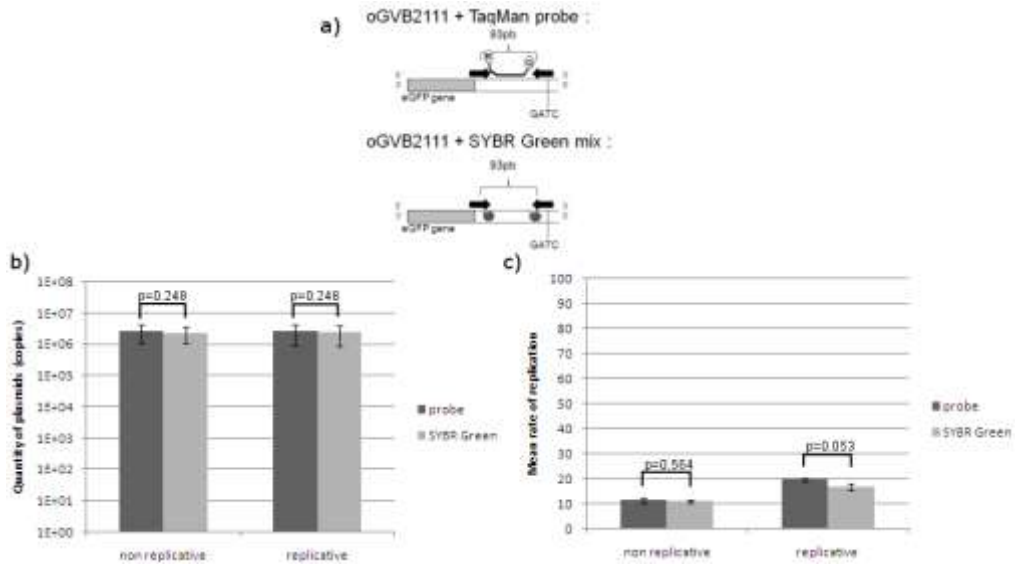
574



575
576 Figure 5
577
578
579
580
581

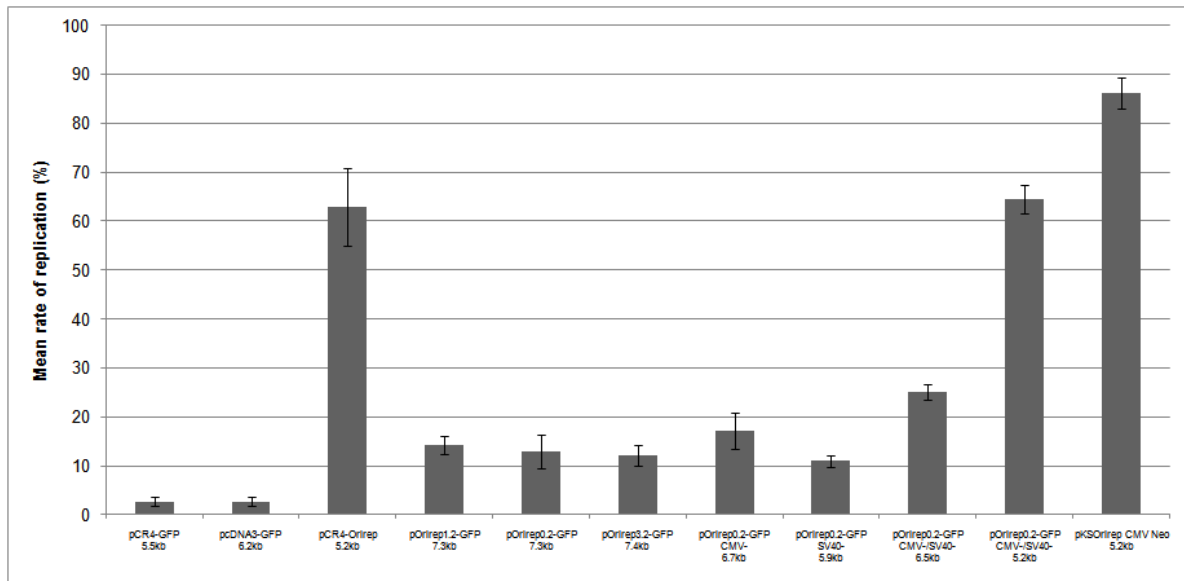


582
583 Figure 6
584



585
586
587
588
589
590
591

Figure 7



592
593
594
595
596

Figure 8